Detection of the neutral MSSM Higgs bosons in the intense-coupling regime at the LHC

E. BOOS¹, A. DJOUADI^{2,3} and A. NIKITENKO⁴

- ¹ Skobeltsyn Institute of Nuclear Physics, Moscow State University, 119992 Moscow, Russia.
 - ² Theory Division, CERN, CH–1211 Geneva 23, Switzerland.
- ³ Laboratoire de Physique Mathématique et Théorique, UMR5825-CNRS, Université de Montpellier II, F-34095 Montpellier Cedex 5, France.
 - ⁴ Imperial College, University of London, London, United Kingdom.

Abstract

We analyse the prospects to detect at the LHC the neutral Higgs particles of the Minimal Supersymmetric Standard Model, when the masses of the two CP-even h, H and of the CP-odd A boson are close to one another, and the value of $\tan \beta$ is large. In this "intense-coupling regime", the Higgs bosons have strongly enhanced couplings to isospin down-type fermions and large total decay widths, so that the $\gamma\gamma$, WW^* and ZZ^* decay modes of the three Higgs bosons are strongly suppressed. We advocate the use of the decays into muon pairs, $h, H, A \to \mu^+\mu^-$, to resolve the three Higgs boson peaks: although the branching ratios are small, $\mathcal{O}(10^4)$, the resolution on muons is good enough to allow for their detection, if the mass splitting is large enough. Using an event generator analysis and a fast detector simulation, we show that only the process $pp \to b\bar{b}\mu^+\mu^-$, when at least one of the b-quarks is detected, is viable.

1. Introduction

The search for the Higgs bosons and the study of their fundamental properties are the primary goals of the LHC. To make sure that Higgs particles with masses in the vicinity of the electroweak scale cannot escape detection, two benchmark models have been studied in great detail: the Standard Model (SM), which predicts the existence of a single Higgs particle H^0 , and its minimal supersymmetric extension (MSSM), where the Higgs sector is extended to contain two CP-even Higgs particles h and H, a CP-odd or pseudoscalar Higgs boson A, and two charged Higgs particles H^{\pm} [1]. In the case of the SM Higgs particle, a plethora of production channels can be used at the LHC and one of the main detection modes is expected to be the gluon–gluon fusion process, $gg \to H^0$, with the signatures $H^0 \to \gamma\gamma$ or $H^0 \to ZZ^{(*)}$, $WW \to 4\ell$ in, respectively, the low and high Higgs boson mass ranges [2].

Because of the complexity of the Higgs spectrum, the situation is more complicated in the MSSM and depends on the values of the two input parameters that characterize the Higgs sector at the tree level, the pseudoscalar Higgs mass M_A and the ratio of the vacuum expectation values of the two Higgs doublet fields $\tan \beta$. It depends also on the mixing in the scalar top sector, which is controlled by the trilinear coupling A_t , when radiative corrections are included [3]. The latter push the maximal value of the lightest h boson from $M_h^{\max} \sim |\cos 2\beta| M_Z \leq M_Z$ at the tree level, to $M_h^{\max} \sim 110$ –130 GeV, depending on the values¹ of $\tan \beta$ and A_t . The MSSM Higgs sector can be divided into three regimes, according to the relative magnitudes of the pseudoscalar Higgs mass M_A and the maximal value of the lightest h boson mass M_h^{\max} . For large $\tan \beta$ values, for which $M_H^{\min} \simeq M_h^{\max}$, the search at the LHC can be summarized as follows [for details, see Ref. [2] for instance]:

- (i) $M_A \gg M_h^{\rm max}$: in this case, we are in the so-called decoupling regime, in which the H,A and H^\pm bosons are very heavy and almost degenerate in mass, $M_A \sim M_H \sim M_{H^\pm}$, while the h boson has a mass $M_h \simeq M_h^{\rm max}$ and SM-like Higgs properties. The techniques devised for the detection of a light H^0 particle can be adapted to the h boson. The A and H bosons, if not too heavy, can be searched for in the channels $gg/q\bar{q} \to b\bar{b}H/A \to b\bar{b}\tau^+\tau^-$, while the H^\pm particle can be detected in the process $gg/q\bar{q} \to t\bar{b}H^- \to t\bar{b}\tau\nu_\tau$ for instance.
- (ii) $M_A < M_h^{\rm max}$: in this case, it is the heavier H boson that will be SM-like, while the h and A particles will be degenerate in mass and couple strongly to b-quarks and τ -leptons for large values of $\tan \beta$. The search techniques are the same as above, except that the roles of the h and H bosons are interchanged. The H^+ particles, because of the MSSM relation $M_{H^\pm} \sim \sqrt{M_A^2 + M_W^2}$, are light enough to be detected in top-quark decays, $t \to H^+b$.
- (iii) $M_A \sim M_h^{\rm max}$: this is what was called the "intense-coupling regime" [6] where the three neutral Higgs bosons have comparable masses, $M_h \simeq M_H \simeq M_A$. The couplings of the CP-even Higgs particles to gauge bosons are both suppressed with respect to the SM [the A boson does not couple to gauge bosons because of CP-invariance], while the h, H and A couplings to down-type (up-type) fermions are strongly enhanced (suppressed).

¹Values $\tan \beta \gtrsim 3$ –10, depending on the mixing in the scalar top sector, are required to maximize the h boson mass and to evade the experimental constraint from LEP2 searches, $M_h \simeq M_A \gtrsim 92$ GeV [4]. From the theoretical viewpoint, very large values of $\tan \beta \sim m_t/m_b \sim \mathcal{O}(50)$ are very interesting, since they allow for Yukawa coupling unification at the Grand Unification scale; see Ref. [5].

While detailed experimental analyses have been performed for the first two scenarios [2], only little work has been done for the intense-coupling regime. In the detailed theoretical discussion given in Ref. [6], it was shown that the search at the LHC might be rather difficult in this regime. The main problem is due to the fact that, for $M_h \sim M_H \sim M_A$ and $\tan \beta \gg 1$, the three neutral Higgs bosons will mainly decay into isospin down-type fermions and the clear $\gamma \gamma$ and ZZ^* , WW signatures cannot be used anymore, the branching fractions being too small. In addition, since the Higgs masses are close, it will be difficult to detect individually the three Higgs bosons, and resolving between the peaks is made even more difficult since the total decay widths can be rather large, implying broader signals.

In this note, we discuss the detection of the three neutral MSSM Higgs bosons $\Phi = h, H, A$ in this scenario, paying a special attention to the possibility of resolving the signal peaks. Performing an event generator analysis that takes into account the signals and the various backgrounds, as well as a simulation of some aspects of one of the LHC detectors [CMS] response, we show that the detection of separate Higgs bosons can be extremely difficult. It can be done only if the Higgs mass differences are sizeable and only if the rare decays into muon pairs, $\Phi \to \mu^+\mu^-$, which have branching ratios at the level of a few times 10^{-4} , are exploited. In addition, the Higgs bosons need to be produced in the associate processes $gg \to b\bar{b}\Phi$, i.e. with at least one b-quark being detected; the processes $gg \to \Phi$ and $b\bar{b} \to \Phi$ suffer from the very large background from Drell–Yan production $pp \to \gamma^*, Z^{(*)} \to \mu^+\mu^-$.

The rest of the discussion is as follows. In the next section, we will recall the main features of the intense coupling scenario. In section 3, we discuss the production of the neutral Higgs bosons and their main backgrounds at the LHC. In section 4, an event generator analysis for the separation of the Higgs bosons is presented. A short conclusion is then given.

2. The intense-coupling regime

As introduced above, the intense-coupling regime is characterized by a rather large value of $\tan \beta$, and a pseudoscalar Higgs boson mass that is close to the maximal (minimal) value of the CP-even h (H) boson mass, $M_A \sim M_h^{\rm max}$, almost leading to a mass degeneracy of the neutral Higgs particles, $M_h \sim M_A \sim M_H$. In the following, we will summarize the main features of this scenario. For the numerical illustration, we will fix the parameter $\tan \beta$ to the value $\tan \beta = 30$ and choose the maximal mixing scenario, where the trilinear Higgs—stop coupling is given by $A_t \simeq \sqrt{6} M_S$ with the common stop masses fixed to $M_S = 1$ TeV; the other SUSY parameter will play only a minor role. The determination of the Higgs masses, couplings and branching ratios is performed using the program HDECAY [7] in which the routine FeynHiggsFast [8] is used for the implementation of the radiative corrections.

The left-hand side of Fig. 1 displays the masses of the MSSM Higgs bosons as a function of M_A , the latter varying from 100 to 140 GeV for our representative value of $\tan \beta$ in the scenario of maximal stop mixing. As can be seen, for M_A close to the maximal h boson mass, which in this case is $M_h^{\rm max} \simeq 130$ GeV, the mass differences $M_A - M_h$ and $M_H - M_A$ are less than about 5 GeV. The H^{\pm} boson mass, given by $M_{H^{\pm}}^2 \sim M_A^2 + M_W^2$, is larger: in the range $M_A \lesssim 140$ GeV, one has $M_{H^{\pm}} \lesssim 160$ GeV, implying that charged Higgs bosons can always be produced in top-quark decays, $t \to H^+b$, and be detected at the LHC.

The couplings of the CP-even Higgs bosons to fermions and gauge bosons normalized to the SM Higgs boson couplings are shown in the right-hand side of Fig. 1 for the same inputs as previously. For small M_A values, the H boson has almost SM couplings, while the couplings of the h boson to W, Z, t (b) are suppressed (enhanced); for large M_A values the roles of h and H are interchanged. For medium values, $M_A \sim M_h^{\rm max}$, the couplings of both h and H to gauge bosons V = W, Z and top quarks are suppressed, while the couplings to b quarks [for which $10 \times g_{\Phi bb}^{-2}$ are shown in the figure] are strongly enhanced. The normalized couplings of the CP-even Higgs particle are simply $g_{AVV} = 0$ and $g_{Abb} = 1/g_{Att} = \tan \beta = 30$.

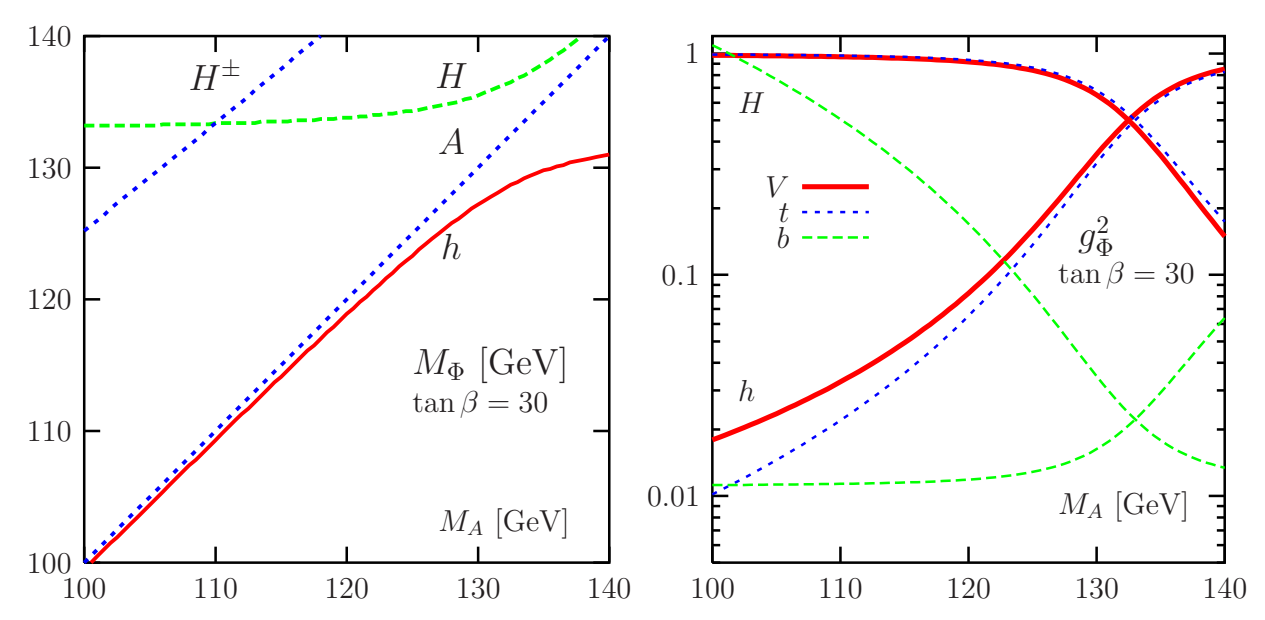


Figure 1: The masses of the MSSM Higgs bosons (left) and the normalized couplings of the CP-even Higgs bosons to vector bosons and third-generation quarks (right) as a function of M_A and $\tan\beta=30$. For the b-quark couplings, the values $10\times g_{\Phi bb}^{-2}$ are plotted.

These couplings determine to a large extent the branching ratios of the Higgs particle decays, which are shown in Fig. 2. Because the couplings of the three Higgs particles to b-quarks and τ -leptons are strongly enhanced, their branching ratios to $b\bar{b}$ and $\tau^+\tau^-$ final are the dominant ones, with values $\sim 90\%$ and $\sim 10\%$ respectively. The decays $H \to WW^*$ do not exceed the level of 10%, even for small M_A values [where H is almost SM-like] and in most of the range displayed for M_A , both the decays $H, h \to WW^*$ are suppressed to the level where they are not useful. The decays into ZZ^* are one order of magnitude smaller. The interesting rare decay mode into $\gamma\gamma$, which is at the level of a few times 10^{-3} in the SM, is very strongly suppressed for the three Higgs particles and cannot be used anymore. Finally, note that the branching ratios for the decays into muons, $\Phi \to \mu^+\mu^-$, are constant in the entire M_A range exhibited, at the level of 3×10^{-4} .

Summing up the partial widths for all decays, the total decay widths of the three Higgs particles are shown in the left-hand side of Fig. 3. As can be seen, for $M_A \sim 130$ GeV, they are at the level of 1–2 GeV, i.e. two orders of magnitude larger than the width of the SM Higgs boson for this value of $\tan \beta$ [the total width increases as $\tan^2 \beta$]. The right-hand side of the figure shows the mass bands $M_{\Phi} \pm \Gamma_{\Phi}$ and, as can be seen, for the above value of M_A , the three Higgs boson masses are overlapping.

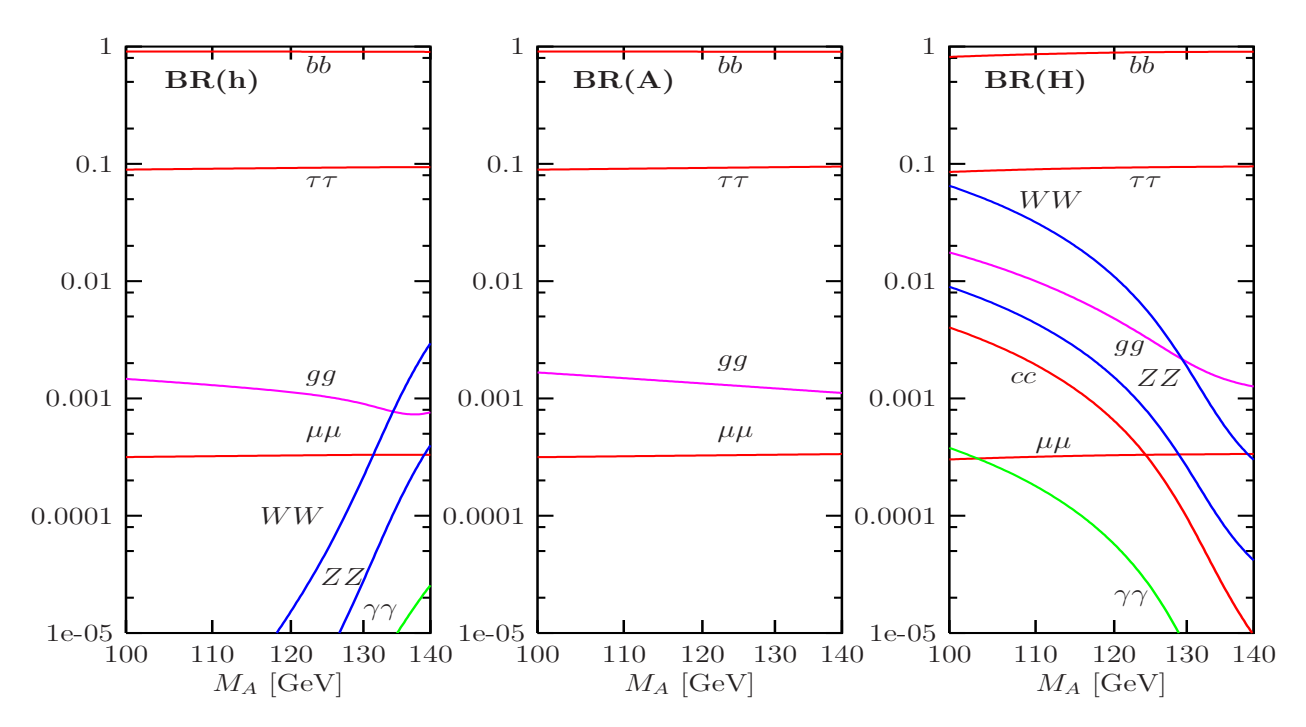


Figure 2: The branching ratios of the neutral MSSM Higgs bosons h, A, H for the various decay modes as a function of M_A and for $\tan \beta = 30$.

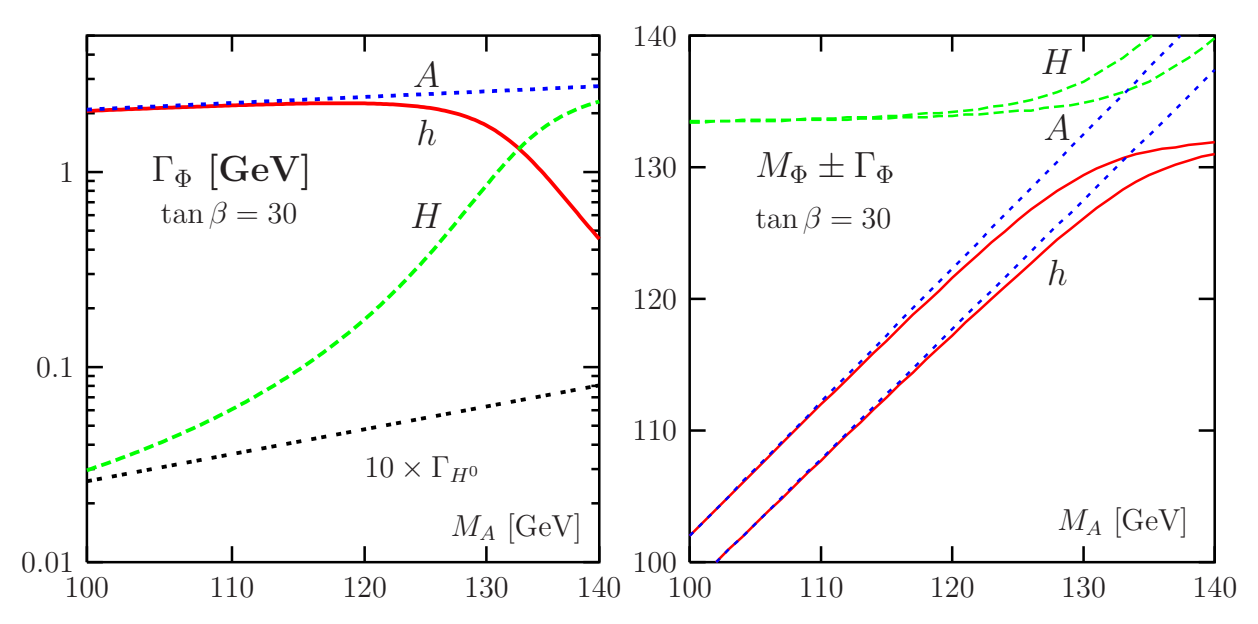


Figure 3: Total decay widths Γ_{Φ} (left) and the mass bands $M_{\Phi} \pm \Gamma_{\Phi}$ (right) for the neutral MSSM Higgs bosons as a function of M_A and for $\tan \beta = 30$.

All these points are summarized for the three values $M_A = 125, 130$ and 135 GeV in Table 1, where we display the Higgs boson masses, their total decay widths and the branching ratios of some important decay modes. These three points, called respectively P1, P2 and P3, are the ones we will choose to perform our analysis of the production and the detection of these Higgs particles at the LHC, the subject to which we now turn our attention.

Point	Φ	M_{Φ}	Γ_{Φ}	$BR(\gamma\gamma)$	$BR(WW^*)$	BR $(\mu^+\mu^-)$
	h	123.3	2.14	1.9×10^{-6}	5.2×10^{-5}	3.29×10^{-4}
P1	A	125.0	2.51	5.9×10^{-7}	0	3.29×10^{-4}
	H	134.3	0.36	2.4×10^{-5}	5.1×10^{-3}	3.31×10^{-4}
P2	h	127.2	1.73	3.7×10^{-6}	2.1×10^{-4}	3.30×10^{-4}
	A	130.0	2.59	4.7×10^{-7}	0	3.31×10^{-4}
	H	135.5	0.85	7.4×10^{-6}	1.9×10^{-3}	3.33×10^{-4}
Р3	h	129.8	0.97	1.0×10^{-5}	9.2×10^{-4}	3.31×10^{-4}
	A	135.0	2.67	4.5×10^{-7}	0	3.33×10^{-4}
	H	137.9	1.69	1.8×10^{-6}	6.5×10^{-4}	3.35×10^{-4}

Table 1: Masses, total widths (in GeV) and some decay branching ratios for the points P1, P2 and P3. The cross sections for the processes $pp \to \Phi$ and $\Phi b\bar{b}$ (in pb) are also shown.

3. Signals and backgrounds at the LHC

As discussed above, the most difficult problem we must face in the intense-coupling regime, is to resolve between the three peaks of the neutral Higgs bosons when their masses are close to one another. The only decays with large branching ratios on which we can rely are the $b\bar{b}$ and $\tau^+\tau^-$ modes. While the former has too large a QCD background to be useful, the latter channel has been shown to be viable for discovery² [2]. However, the expected experimental resolution on the invariant mass of the $\tau^+\tau^-$ system, in the mass range that we are interested in, is of the order of 10 to 20 GeV, and thus clearly too large to resolve the three Higgs peaks. One would then simply observe a relatively wide resonance corresponding to A and h and/or H production. Since the branching ratios of the decays into $\gamma\gamma$ and $ZZ^* \to 4\ell$ are too small, a way out is to use the Higgs decays into muon pairs: although the branchings ratio are rather small, BR($\Phi \to \mu^+\mu^-$) $\sim 3.3 \times 10^{-4}$, the resolution is expected to be as good as 1 GeV, i.e. comparable to the total width, for $M_{\Phi} \sim 130$ GeV.

Because of the strong enhancement of the Higgs couplings to bottom quarks, the three Higgs bosons will be produced at the LHC mainly in the gluon–gluon process

$$gg \to \Phi = h, H, A \to \mu^+ \mu^-$$
, (1)

which is dominantly mediated by b-quark loops, and the associated production with $b\bar{b}$ pairs,

$$gg/q\bar{q} \to b\bar{b} + \Phi = h, H, A \to b\bar{b} + \mu^+\mu^-$$
 (2)

The Higgs-strahlung $pp \to HV$ and vector-boson fusion $qq \to Hqq$ processes, as well as associated production with top quarks, will have smaller cross sections than for the SM Higgs boson since the couplings to the involved particles are suppressed. The two processes eqs. (1) and (2) have recently been discussed in Refs. [9] and [10], respectively, and have

²Note that in previous CMS analyses of the $pp \to b\bar{b} + \mu^+\mu^-$ signature, the complete 4-fermion background was not been fully included. This remark applies also to the $pp \to b\bar{b} + \tau^+\tau^-$ signature.

been shown to be viable for the discovery of relatively light Higgs bosons³.

For the calculation of the signal cross sections for the $pp \to \mu^+\mu^-$ final state, since they give rise to the same topology, we sum the cross sections of both the $gg \to \Phi \to \mu^+\mu^-$ process and the $gg/q\bar{q} \to b\bar{b} + \Phi$ process where the transverse momenta of the b-quarks are too small , $p_{\perp}^{b,\bar{b}} \leq 20$ GeV, to be detected. For the former process, we apply a K-factor of 1.7 [13] to take into account the NLO QCD corrections, while for the latter one, we apply a K-factor of 1.5 to the LO cross section evaluated at a scale $\mu \sim \frac{1}{2}M_H$ as recently reported in Ref. [17]. One then obtains production rates at the level of a fraction of a picobarn for $pp \to h, H, A \to \mu^+\mu^-$. For the process $gg \to \Phi b\bar{b}$, where we require the two bottom quarks to be detected, i.e. with $p_{\perp}^{b,\bar{b}} \geq 20$ GeV, the NLO cross section is approximately the same as the LO cross section when it is evaluated at the scale $\mu = M_H/2$ and a running b-quark mass for the bottom Yukawa coupling [17]. The obtained cross sections in this case are one order of magnitude smaller than those of the inclusive $pp \to \Phi \to \mu^+\mu^-$ case.

For the backgrounds to $\mu^+\mu^-$ production, we have included only the Drell-Yan process $pp \to \gamma^*, Z^* \to \mu^+\mu^-$, which is expected to be the largest source [as will be seen later, this is sufficient for our conclusion]. For the $pp \to \mu^+\mu^-b\bar{b}$ final state, however, we have included the full 4-fermion background, which is mainly due to the process $pp \to b\bar{b}Z$ with $Z \to \mu^+\mu^-$. Both signals and backgrounds have been generated with the program CompHEP [18].

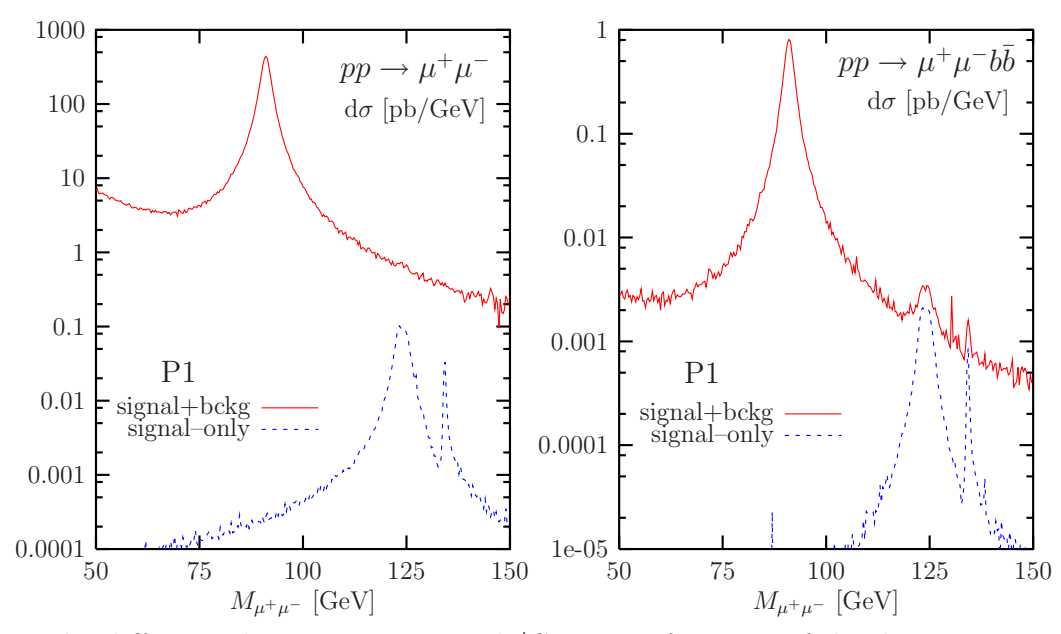


Figure 4: The differential cross section in pb/GeV as a function of the dimuon mass for the point P1, for both the signal and signal plus background in the processes $pp(\to \Phi) \to \mu^+\mu^-$ (left figure) and $pp(\to \Phi b\bar{b}) \to \mu^+\mu^- b\bar{b}$ (right figure).

³The vector-boson fusion process $qq \to H^0 \to \mu^+\mu^-$ has also been considered for a SM Higgs boson [11] and has been shown to work at the LHC only if an unreasonable amount of luminosity is collected. In addition, the process $qq \to h, H \to \tau^+\tau^-$ discussed in Ref. [12] cannot be used to resolve the two h and H peaks in the intense-coupling regime, because of the poor resolution on the $\tau^+\tau^-$ invariant mass.

⁴Note that the cross section calculated directly for bottom-quark fusion $b\bar{b} \to \Phi$ at NNLO [14] gives approximately the same results if the factorization and the renormalization scales are chosen properly, as it was shown in Refs. [15, 16].

The differential cross sections are shown for the scenario P1 as a function of the invariant dimuon mass in the left-hand side of Fig. 4, for the final state $pp(\to h, H, A) \to \mu^+\mu^-$. As can be seen, the signal rate is fairly large and we may hope, in principle, to see two peaks: one corresponding to the production of the h/A bosons and one to the production of the H boson. However, when put on top of the huge Drell–Yan background, the signal becomes completely invisible. This holds true even with some optimization of the cuts; for instance, applying a cut on the muon transverse momenta $p_{\perp}^{\mu} \geq 50$ GeV, which should strongly suppress the Drell–Yan cross section, still leaves too large a background. The same features hold for the points P2 and P3, and we conclude, contrary to Ref. [9], that already at the level of a "theoretical simulation", the Higgs boson signal in the inclusive $pp \to \mu^+\mu^-$ process will probably be hopeless to extract for Higgs masses below 140 GeV, unless unreasonably large values of the parameter tan β are chosen to enhance the signal rate.

In the right-hand side of Fig. 4, we display, again for scenario P1, the signal cross section from $pp \to \mu^+\mu^-b\bar{b}$ and the complete 4-fermion SM background cross section as a function of the dimuon system. The number of signal events is an order of magnitude smaller than in the previous case, but one can still see the two peaks. However, the main difference here is that the rate for the background is much smaller than in the Drell–Yan case. Once the signal events are put on top of the background distribution, one can still see the two peaks corresponding to h/A and H production. The same analysis has been repeated for scenarios P2 and P3, and the output for the signal and background rates is shown in Fig. 5. As can be seen, the situation is similar to that of the previous case, except that here the mass difference between the Higgs bosons is large enough for us to hope that the three individual peaks could be resolved.

Note, however, that up to now, we did not include any efficiency for the detection of b quarks and muons and did not assume any resolution for the mass of the dimuon system.

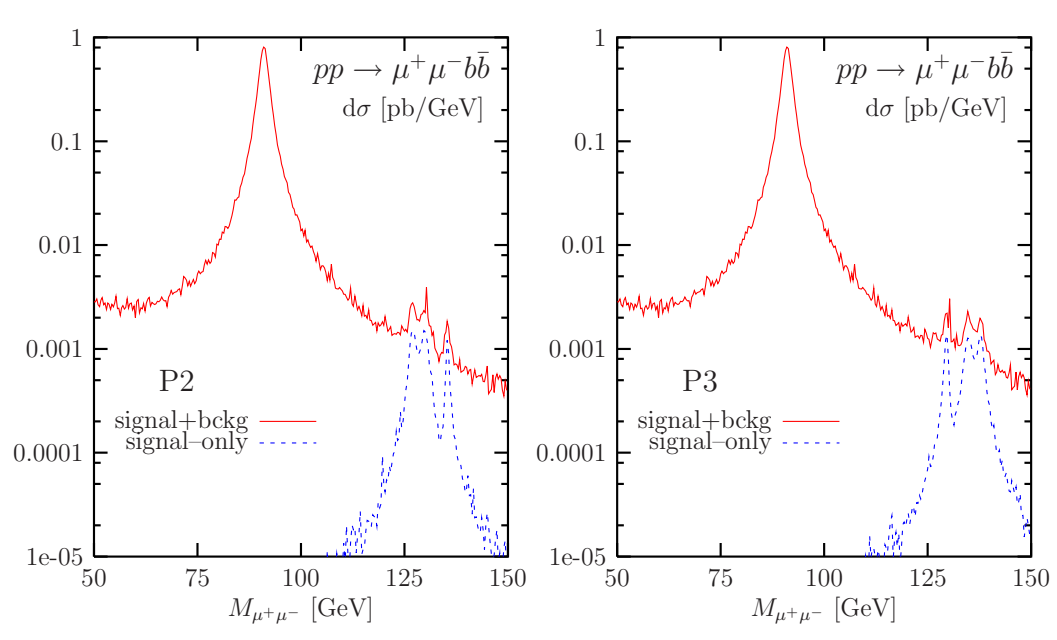


Figure 5: The differential cross section in pb/GeV as a function of M_A for both the signal and signal plus background in the process $pp(\to \Phi b\bar{b}) \to \mu^+\mu^-b\bar{b}$ for P2 (left) and P3 (right).

4. An event generator analysis

In order to perform a more realistic analysis, we have generated unweighted events for the full 4-fermion background $pp \to \mu^+\mu^- + b\bar{b}$ and for the signal, for the three parameter points P1, P2 and P3 already introduced; as above, the generator CompHEP has been used. With the help of the new CompHEP-PYTHIA interface [19], which has been upgraded to include the implementation of the so-called Les Houches Accord 1 [20], the unweighted events have been processed through PYTHIA 6.2 [21] for fragmentation and hadronization, taking into account initial- and final-state radiation. We stress, once more, that the requirement of observing both b-jets, with $p_{\perp}^{b,\bar{b}} > 20$ GeV, leads to a reduction by a factor of 10 of the signal rate compared to the fully inclusive case. In turn, the background reduction factor in this case is about 200, resulting in a much larger $S/\sqrt{S+B}$ than in the inclusive case; see Fig. 4.

To simulate detector effects, such as acceptance, muon momentum smearing, and b-jet tagging, we take the example of the CMS detector. Using the CMSJET package [22], in which muon momentum smearing has been parametrized from a full simulation of the CMS tracker layout as described in Ref. [23], a mass resolution of about 1% on the dimuons from the Higgs decays is obtained. The events are assumed to be triggered by a double muon trigger, with a 7 GeV threshold and within an acceptance of $|\eta| < 2.1$, leading to an efficiency of 97% per muon [24]. For b-jet tagging, we use the b-tagging efficiency obtained by the technique described in Ref. [25]. This technique, developed for tagging soft jets of 20–30 GeV, does not require the b-jet reconstruction in the calorimeter, but exploits the tracker information [only searching for vertex and tracks with significant impact parameter]. With a full detector simulation, such a method gives 40% efficiency per $gg \rightarrow b\bar{b}$ + Higgs event for a Higgs boson mass of 150 GeV.

The results of the simulation for an integrated luminosity of 100 fb⁻¹ are shown in Fig. 6. As expected, the signal invariant mass distributions become broader, even with the good CMS momentum resolution. This is shown in the plots of Fig. 6, where the number of $\mu^+\mu^-b\bar{b}$ events in bins of 0.25 GeV are shown as a function of the mass of the dimuon system. The left-hand side shows the signals with and without the resolution smearing as obtained in the Monte-Carlo analysis, while the figures in the right-hand side show also the backgrounds, including the detector effects.

For point P1, the signal cross section for the heavier CP-even H boson is significantly smaller than the signals from the lighter CP-even h and pseudoscalar A bosons; the latter particles are too too close in mass to be resolved, and only one single peak for h/A is clearly visible. To resolve also the peak for the H boson, the integrated luminosity should be increased by a factor of 3 to 4. In the case of point P2, it would be possible to see also the second peak, corresponding to the H boson signal with a luminosity of 100 fb⁻¹, but again the h and A peaks cannot be resolved. In the case of point P3, all three h, A and H bosons have comparable signal rates, and the mass differences are large enough for us to hope to be able to isolate the three different peaks, although with some difficulty.

Note that, if the $\tau^+\tau^-$ final-state decays of the Higgs bosons had been used, with the expected resolution on τ leptons, we would have seen only one broad resonance and could not have resolved even two signal peaks in all three scenarios.

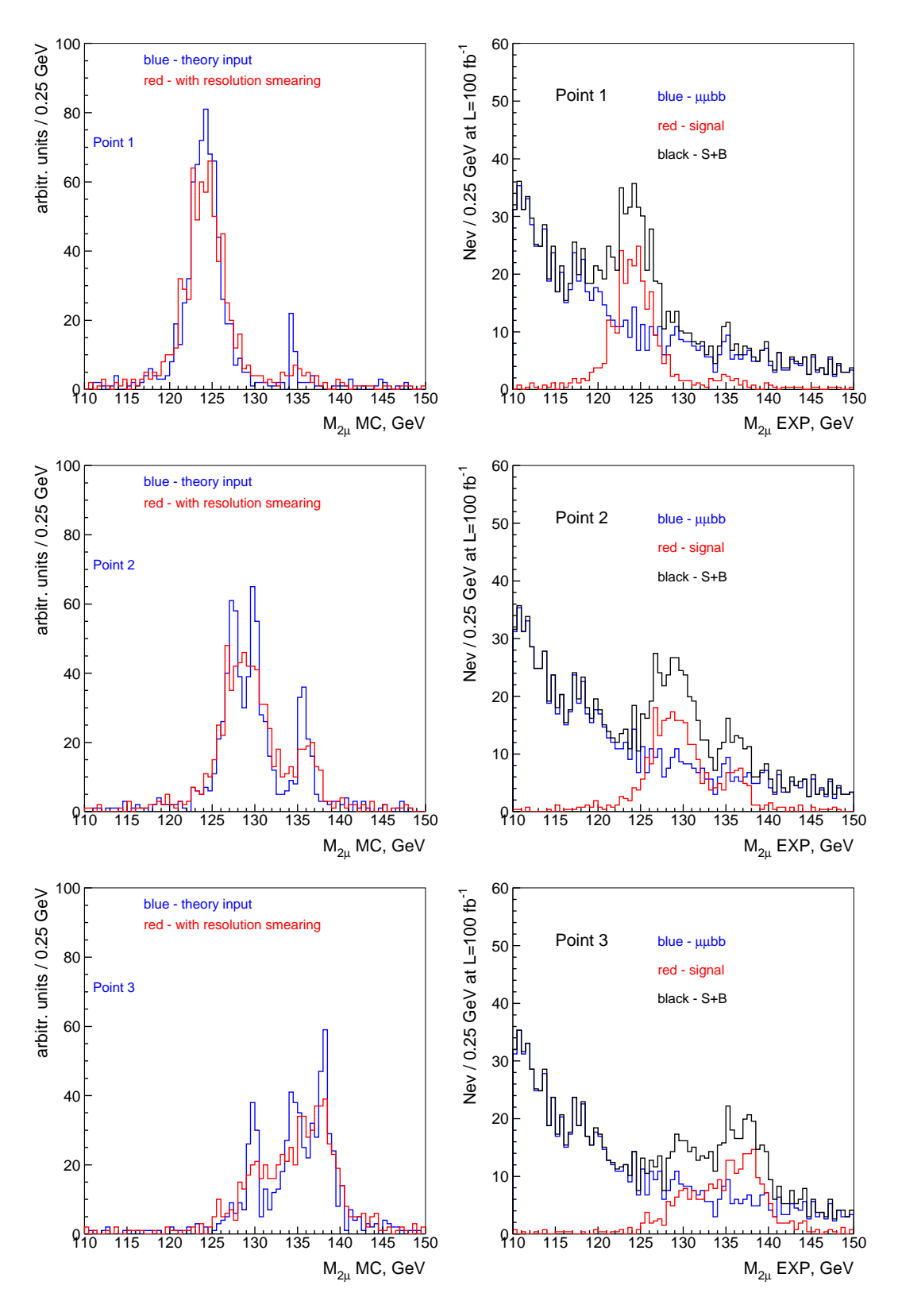


Figure 6: $\mu^+\mu^-$ pair invariant mass distributions for the signal before and after detector resolution smearing (left) and for the signal and the background (right) for P1, P2 and P3 parameter points.

5. Conclusions

We have shown that in the intense-coupling regime, i.e. when the h, H and A MSSM bosons have masses too close to the critical point M_h^{max} and when the value of $\tan \beta$ is large, the detection of the individual Higgs boson peaks is very challenging at the LHC. It is only in the associated Higgs production mechanism with $b\bar{b}$ pairs, with at least one tagged b-jet, and with Higgs particles decaying into the clean muon-pair final states, that there is a chance of observing the three signals and resolve between them⁵. This would be possible only if the Higgs mass differences are larger than 3–5 GeV.

In the present note, we only concentrated on the fully exclusive $b\bar{b} + \mu^+\mu^-$ signature, requiring both b-jets to be observed, and included only the irreducible 4-fermion background, which is expected to be the dominant one. In a more complete study, one should eventually consider the case where only one single b-jet is tagged, which should increase the cross section signal [15], and take into account also the reducible backgrounds from $pp \to Z^*/\gamma^* \to \mu^+\mu^-$ with mistagged jets [which is expected to be large in this case] as well as other backgrounds. Such a study is beyond the scope of this note and will appear elsewhere [27].

Acknowledgments: We thank John Campbell, Michael Kramer, Tilman Plehn, Laura Reina, Michael Spira and Scott Willenbrock for very lively discussions on the $b\bar{b}$ + Higgs process, during and after the Les Houches Workshop. Discussions with Daniel Denegri and Elzbieta Richter-Was are also acknowledged. EB is partly supported by the INTAS 00-0679, CERN-INTAS 99–377 and Universities of Russia UR.02.03.002 grants.

References

- [1] For a review on the Higgs sector of the MSSM, see J.F. Gunion, H.E. Haber, G.L. Kane and S. Dawson, "The Higgs Hunter's Guide", Addison-Wesley, Reading, 1990.
- [2] CMS Collaboration, Technical Proposal, report CERN/LHCC/94-38 (1994); ATLAS Collaboration, Technical Design Report, CERN/LHCC/99-15 (1999); J.F. Gunion, A. Stange and S. Willenbrock, in "Electroweak symmetry breaking and new physics at the TeV scale", hep-ph/9602238; Proceedings of the Les Houches Workshops "Physics at TeV colliders", A. Djouadi et al., hep-ph/0002258 (1999) and D. Cavalli et al., hep-ph/0203056 (2001).
- [3] S. Heinemeyer, W. Hollik and G. Weiglein, Eur. Phys. J. C9 (1999) 343; M. Carena et al.,
 Nucl. Phys. B580 (2000) 29; J.R. Espinosa and R.J. Zhang, Nucl. Phys. B586 (2000)3;
 G. Degrassi, P. Slavich and F. Zwirner, Nucl. Phys. B611 (2001) 403; A. Brignole, G. Degrassi, P. Slavich and F. Zwirner, Nucl. Phys. B631 (2002) 195 and B643 (2002) 79.
- [4] The LEP Higgs working group, hep-ex/0107029 and hep-ex/0107030.

⁵Very recently, it has been argued that in central diffractive Higgs production, $pp \to p + \Phi + p$, the cross section for A production is very small, and these processes could allow to discriminate between h and H production since, with forward proton taggers, a very small mass resolution can be obtained [26].

- V. Barger, M.S. Berger, P. Ohmann and R.J.N. Phillips, Phys. Lett. B314 (1993) 351;
 M. Carena, S. Pokorski and C. E. M. Wagner, Nucl. Phys. B406 (1993) 59.
- [6] E. Boos, A. Djouadi, M. Mühlleitner and A. Vologdin, Phys. Rev. D66 (2002) 055004.
- [7] A. Djouadi, J. Kalinowski and M. Spira, Comput. Phys. Commun. 108 (1998) 56.
- [8] S. Heinemeyer, W. Hollik and G. Weiglein, CPC 124 (2000) 76 and hep-ph/0002213.
- [9] V. Barger and C. Kao, Phys. Lett. B424 (1998) 69; Tao Han and B. McElrath, Phys. Lett. B528 (2002) 81.
- [10] S. Dawson, D. Dicus and C. Kao, Phys. Lett. B545 (2002) 132.
- [11] T. Plehn and D. Rainwater, Phys. Lett. B520 (2001) 108.
- [12] T. Plehn, D. Rainwater and D. Zeppenfeld, Phys. Lett. B454 (1999) 297.
- [13] M. Spira, A. Djouadi, D. Graudenz and P.M. Zerwas, Phys. Lett. B318 (1993) 347 and Nucl. Phys. B453 (1995) 17.
- [14] R. Harlander and W. Kilgore, hep-ph/0304035.
- [15] J. Campbell, R.K. Ellis, F. Maltoni and S. Willenbrock, Phys. Rev. D67 (2003) 095002.
- [16] E. Boos and T. Plehn, hep-ph/0304034 (to appear in Phys. Rev. D).
- [17] Talks given by M. Kraemer and L. Reina, at the Les Houches Workshop, June 2003.
- [18] A. Pukhov, E. Boos, M. Dubinin, V. Edneral, V. Ilyin, D. Kovalenko, A. Kryukov, V. Savrin, S. Shichanin and A. Semenov, Report INP-MSU 98-41/542, hep-ph/9908288.
- [19] A.S. Belyaev et al., "CompHEP-PYTHIA interface: Integrated package for the collision events generation based on exact matrix elements", hep-ph/0101232.
- [20] E. Boos et al., "Generic user process interface for event generators", hep-ph/0109068.
- [21] T. Sjöstrand, L. Lönnblad and S. Mrenna, "PYTHIA 6.2: Physics and manual", hep-ph/0108264.
- [22] S. Abdullin, A. Khanov and N. Stepanov, CMS Note-1994/180.
- [23] The Tracker Project TDR, CERN/LHCC 98-6, CMS TDR 5, 15 April 1998.
- [24] The Trigger and Data Acquisition Project, Volume II, CERN/LHCC 2002-26, CMS TDR 6.2, 15 December 2002.
- [25] L. Belluci, "MSSM Neutral Higgs Boson searches at CMS in the $\mu\mu$ channel", Dissertation, Universita degli studi di Firenze, December 2001.
- [26] A. Kaidalov, V. Khoze, A. Martin and M. Ryskin, hep-ph/0307064.
- [27] E. Boos et al., in progress.